IEEE Access
Multidisciplinary : Rapid Review : Open Access Journal

Received 18 November 2023, accepted 8 December 2023, date of publication 12 December 2023, date of current version 18 December 2023.

Digital Object Identifier 10.1109/ACCESS.2023.3342049

RESEARCH ARTICLE

Joint Power Allocation Algorithm for UAV-Borne Simultaneous Transmitting and Reflecting Reconfigurable Intelligent Surface-Assisted Non-Orthogonal Multiple Access System

YI PENG[1,2], JIAN TANG[1,2], QINGQING YANG[1,2], ZHUOTING HAN[1,2], AND JIAN MA[1]
[1]College of Information Engineering and Automation, Kunming University of Science and Technology, Kunming 650500, China
[2]Yunnan Key Laboratory of Computer Science, Kunming University of Science and Technology, Kunming 650500, China

Corresponding author: Qingqing Yang (1085596741@qq.com)

This work was supported by the National Natural Science Foundation of China under Grant 61761025.

ABSTRACT As a novel technology, simultaneous transmitting and reflecting reconfigurable intelligent surface (STAR-RIS) provides users with full spatial coverage communication by modulating reflected and refracted signals. This study proposes a novel UAV equipped with STAR-RIS-assisted non-orthogonal multiple access system that jointly optimized the cluster correlations with the power allocation coefficients and positions of STAR-RIS to maximize the user system sum rate. However, the application of this technique is limited by the complex nonconvex optimization problem, which was addressed by developing an alternating optimization iteration algorithm. The joint optimization problem related to cluster association and the power allocation coefficients and positions of STAR-RIS was solved by alternating iterations. The simulation results demonstrated that the proposed algorithm delivered a superior user system sum rate compared to single-power optimization, ultimately achieving near-optimal system performance. At the same time, we verified that the NOMA system equipped with STAR-RIS on UAV can achieve the best performance than the OMA system. Therefore, the proposed algorithm contributes to the optimization of STAR-RIS-assisted systems, which will benefit applications in wireless communications, IoT, and smart city infrastructure.

INDEX TERMS Simultaneous transmitting and reflecting reconfigurable intelligent surface, unmanned aerial vehicle, power allocation, non-orthogonal multiple access, position deployment.

I. INTRODUCTION

Reconfigurable intelligent surface (RIS) is an advanced communication technology for sixth-generation (6G) wireless communication, which can be used to provide higher-frequency spectrum and higher energy efficiency [1]. The introduction of intelligent reflective surfaces (IRS) has improved the quality of communication services in non-line-of-sight (NLOS) cells [2]. In general, conventional IRS are affixed to the walls of tall buildings and display only reflective capability. Therefore, users within the reflective range of the IRS are benefitted from high-quality service. However, users on the rear side of the IRS experience a higher probability of disruption or link outage. To solve this communication problem, a new IRS-simultaneous transmitting and reflecting RIS (STAR-RIS)-has been developed to improve the quality of service for the users located on the rear side of the IRS [3].

Compared with conventional IRS that can only serve hemispherical users, STAR-RIS achieves a higher range of service area, allows greater flexibility in designing the beam formation for reflection and refraction, and can provide 360° coverage [4]. Therefore, unmanned aerial vehicle (UAV)-borne STAR-RIS can moderate the reflection of the incident

The associate editor coordinating the review of this manuscript and approving it for publication was Mohamed M. A. Moustafa.

signal and height adjustment of the STAR-RIS, thereby improving the strength and quality of the communication signal. Moreover, the STAR-RIS-assisted UAV communication system can dynamically adjust the direction and amplitude of the reflective surface according to the communication needs of various environments. Therefore, it can more readily adapt to the UAV flight trajectory and communication environment to deliver improved communication performance.

A. RELEVANT WORK

1) STAR-RIS-RELATED RESEARCH

A previous study [3] proposed three operational protocols applicable to STAR-RIS: energy-splitting (ES), mode-switching (MS), and time-switching (TS) protocols. Subsequently, the design of efficient uplink channel estimation for STAR-RIS-assisted dual-user communication systems was investigated [5]. The numerical results verified that STAR-RIS yielded a smaller channel estimation error under the TS protocol than under the ES protocol. The resource allocation issue in STAR-RIS-supported multicarrier communication networks was investigated through a study. The study [6] entailed the development of joint optimization algorithms for channel allocation, power allocation, and transmission and reflection beamforming for STAR-RIS to attain the highest user sum rate possible. The simulation results obtained from this study revealed that the STAR-RIS-supported non-orthogonal multiple access (NOMA) system performed significantly better than the system utilizing conventional RIS and orthogonal multiple access (OMA).

A recent academic investigation, cited as [7], has presented an evaluation regarding the probability of network interruption for STAR-RIS-supported NOMA networks transmitting data through spatially correlated channels. The study has concluded that the total data transmission has been optimized by a comprehensive refinement of various factors including the decoding sequence, power allocation coefficient, active beamforming, and transmission and reflection beamforming, as jointly determined by the researchers, as presented in [8]. The proposed STAR-RIS-NOMA system has been demonstrated to exhibit superior performance compared to conventional RIS-NOMA and RIS-assisted OMA systems, as evidenced by simulation validation. In related studies, researchers [9] have undertaken optimization of the reflection and transmission coefficients of STAR-RIS elements with a view to enhancing the performance of the system in both ES and MS protocols, with a specific focus on maximizing the weighted sum rate.In reference [10], the author developed a heterogeneous multi-agent system for solving distributed constraint optimization problems in an undirected network. They designed an adaptive control algorithm based on the Karush-Kuhn-Tucker (KKT) conditions and primal-dual control structure. Simulation results demonstrate that the proposed algorithm converges to the optimal solution of the distributed resource allocation problem, considering both state and output information.

2) UAV-BORNE STAR-RIS RESEARCH

As STAR-RIS is mounted on high buildings, its communication coverage is preset. UAV-borne STAR-RIS can be deployed mobile to completely utilize the benefits of STAR-RIS. Literature [11] proposes a set of low-cost passive metasurfaces dynamically deployed by a swarm of drones to create cascade channels to improve user services and security enhancement. In a recent research work [4], a problem was formulated to maximize the sum rate of a system that involves the joint optimization of the trajectory of an unmanned aerial vehicle (UAV), the formation of an active beam by the UAV, and the formation of a passive transmission/reflection beam by the space-terrestrial aerial radio-frequency integrated system (STAR-RIS). To address this problem, reinforcement learning (RL) was employed to optimize the UAV trajectory and the active and passive beamforming in a simultaneous manner. The simulation and validation results clearly indicate that the use of STAR-RIS in conjunction with UAV communication leads to a significant increase in the sum rate, as compared to the conventional RIS that relies solely on reflection. In addition, a quantum sensing-phantom imaging-based beam training method is proposed for STAR-RIS-assisted terahertz-level multi-user large-scale multiple-input-multiple-output system in another study [12]. This scholarly work examines the joint investigation of several key factors, including the proposed BS sub-array and sub-star spatial multiplexing structure, optimal active and passive beam formation, digital precoding, and optimal position of the UAV, in an effort to maximize the average reachable sum rate of users. The simulation results demonstrate that this scheme effectively achieves beam training and separation channel estimation, leading to a significant improvement in spectral efficiency. In addition, the total rate for all users was maximized by jointly optimizing the beamforming vector, UAV trajectory, and power allocation of STAR-RIS [13]. The relevant simulation results verified that the UAV-assisted STAR-RIS completely utilized the advantages of STAR-RIS and achieved higher sum rates.However, the UAV used in the literature [12] is equipped with a STAR-RIS structure. During the flight of the UAV, the STAR-RIS moves with the movement of the UAV, which will bring more air to the UAV. drag and impairs the aerodynamic performance of the drone.

Therefore, the challenge for UAVs equipped with STAR-RIS is how to optimize the structure of the UAV without compromising the aerodynamic performance of the UAV, and ultimately maximize the user's safety and speed.However, in reference [12], the unmanned aerial vehicle (UAV) is equipped with a STAR-RIS structure, which moves along with the UAV during its flight. This movement introduces additional aerodynamic drag and potentially hampers the aerodynamic performance of the UAV. Therefore, the challenge of mounting STAR-RIS on UAVs lies in optimizing the UAV's structure without compromising its aerodynamic performance, ultimately achieving user rate maximization.

B. MOTIVATIONS AND CONTRIBUTIONS

The utilization of the STAR-RIS technology in wireless communication networks has been shown to provide numerous benefits:

(1) The communication coverage throughout a given space can be expanded by means of simultaneously transmitting and reflecting incident signals.

(2) STAR-RIS provides considerable freedom for system design and facilitates the optimization of cluster association relationships and power allocation factors.

(3) The utilization of Unmanned Aerial Vehicles (UAVs) incorporating the STAR-RIS technology enables the agile adaptation of STAR-RIS positioning in response to user distribution, thereby significantly augmenting the overall mobility of STAR-RIS.

Thus, an integrated optimization of the STAR-RIS position, user cluster correlations, and power allocation factors is imminent for completely leveraging the potential of STAR-RIS. However, this non-convex problem is extremely challenging owing to the highly coupled nature of the optimization variables. Therefore, the integrated optimization of these variables is a critical step for STAR-RIS-assisted NOMA systems. As the number and size of user clusters depend on the type of user distribution and communication environment, the joint optimization procedure must consider multiple types of user distribution.

This study aims to address a research gap in the field of UAV-borne STAR-RIS-assisted NOMA system design. Specifically, to the best of our knowledge, no prior research has undertaken a joint optimization approach to this design. Thus, through an extensive investigation, this study seeks to make contributions to the field by filling this gap and offering novel insights into this topic:

(1) Joint power allocation for UAV-borne STAR-RIS-assisted NOMA systems is investigated. In the considered STAR-RIS-NOMA network, a base station can communicate with two users located on each side of the STAR-RIS, and the communication between the base station and the users relies only on the STAR-RIS. In addition, the STAR-RIS works with an MS protocol, which ensures the complete reflection or transmission of all components.

(2) The original problem is segmented into three subproblems, which were subjected to alternant solution by considering two sets of variables. In the cluster association problem, an improved Harris Hawk optimization algorithm (IHHO) was employed to solve the component load discrepancy problem. Furthermore, we proposed a continuous convex approximation power allocation algorithm based on the interior point method to solve the power allocation problem. An improved artificial fish swarm algorithm was used to select the optimal deployment position, thereby solving the position deployment problem of STAR-RIS.

According to the simulation results, the proposed alternating iteration algorithm could effectively solve the power allocation problem by combining the cluster association relationship with position deployment, eventually attaining a near-optimal system performance. The experimental results show that our proposed algorithm has better performance in NOMA system than OMA system.

C. PAPER STRUCTURE

The remainder of the paper is structured as follows. In Section II, the structural model, the system model and communication model of UAVs equipped with STAR-RIS are briefly described. The alternating iterative joint optimization algorithm is proposed in Section III, and the simulation results are discussed in Section IV. Finally, the conclusions are summarized in Section V.

II. MODEL CONSTRUCTION

A. NEW UAV EQUIPPED WITH STAR-RIS MODEL

Literature [14] studies the issues that need to be considered when carrying RIS on a UAV, including path loss model, maneuverability, etc. For this reason, we redesigned the structure of a new type of UAV equipped with STAR-RIS.As shown in the Figure 1, we have newly designed a structure for UAV equipped with STAR-RIS panels. We use a large quadrotor drone for modification. The lower frame is pulled by a set of foldable telescopic rods, and the STAR-RIS panel is inside the frame. RIS. When the UAV takes off to the destination point that needs to be relayed, the telescopic rod is in a retracted state and remains parallel to the bottom of the UAV to ensure that no more air resistance is applied to the UAV during flight; when at the destination When clicked, the telescopic rod is in an extended state and is perpendicular to the bottom of the drone. This new UAV structure can reduce the air resistance of the UAV during flight and can better meet the communication needs of UAV equipped with STAR-RIS.

During flight, STAR-RIS is in a contracted state and parallel to the drone. We assume that the air, wind speed and pressure are at normal levels, and the drag coefficient of the drone carrying STAR-RIS is considered negligible.

The telescopic pole is powered and controlled by the UAV, requiring less electricity. In order to completely solve the concerns about UAV power, Tyrovolas [15] proposed a future Internet of Things network data collection scheme based on UAVs carrying RIS, and analyzes the performance of the scheme from two aspects: coverage and average collected data, in order to improve the energy efficiency of the network. Yang [16] studied an unmanned aerial vehicle wireless communication system with energy harvesting function, which can minimize the total energy consumption of the UAV while meeting the user's minimum data transmission requests. Xiao [17] designed a solar UAV structure equipped with RIS, which uses solar energy to power the UAV.

B. SYSTEM MODEL

The communication scenario is illustrated in Figure 2. The UAV-borne STAR-RIS provides communication services to E ground users in the target area. The number of antennas at the

(a) UAV-borne with fold STAR-RIS in the folded state

(b) UAV-borne with fold STAR-RIS in the unfolded state

FIGURE 1. UAV-borne with fold STAR-RIS.

base station is J. The STAR-RIS is configured with a Uniform planar array (UPA) containing $M * N$ reflective units, where the phase of each reflective unit is controlled by the UAV. Presumably, the reflecting and refracting users are paired at various power levels in the same resource block in case the direct link between two NOMA users and the base station is disrupted, i.e., if the direct link between the reflecting user and the base station is obstructed by an obstacle (trees or tall buildings). Therefore, the signal from the base station can be reflected only by the UAV-borne STAR-RIS. As the refractive users are located behind the STAR-RIS substrate, they cannot access any reflective link. Owing to the superiority of the STAR-RIS, the signal can be refracted through the substrate, which is the only link through which the refracted user can receive the signal from the base station. In summary, the base station first transmits the signal to the STAR-RIS that subsequently reflects or refracts the signal to the reflecting and refracting users.

Here, the set of components is denoted as $A = \{a_1, a, \cdots, a_M\}$; the set of the number of beams per component is represented as $B = \{b_1, b, \cdots, b_M\}$; the number of clusters of users can be expressed as $c = \{c_1, c, \cdots, c_S\}$; and the number of users is denoted by $E = \{e_1, e_2, \cdots, e_E\}$.

C. COMMUNICATION MODEL

Herein, we considered a UAV-borne STAR-RIS-assisted NOMA system, assuming that the base station in the cell is damaged, and communication can be executed only by the external base stations. The link between the base station and the user cannot using owing to the distance and obstacles, necessitating the use of UAV-borne STAR-RIS for relay communication. The link between the base station and the

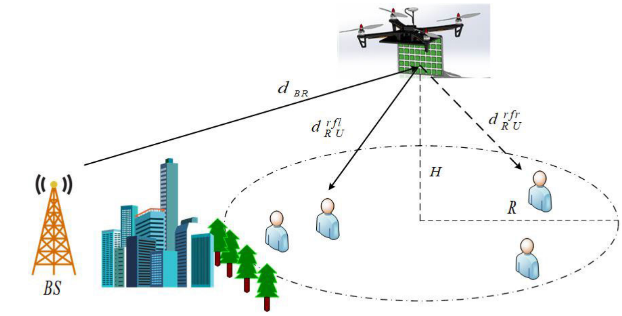

FIGURE 2. UAV-borne STAR-RIS assisted NOMA communication system model.

UAV-mounted STAR-RIS can be regarded as a line-of-sight link.

Thus, we presumed that the horizontal position of the base station and STAR-RIS was $w_{BS} = [x_{BS}, y_{BS}]^T$ and $w_R = [x_R, y_R]^T$, respectively, and their corresponding height was H_{BS} and H_R, respectively. Moreover, the horizontal positions of the reflective user and the refractive user could be expressed as $w_{rfl} = \left[x^u_{rfl}, y^u_{rfl}\right]^T (1 \leq u \leq U)$ and $w_{rfr} = \left[x^k_{rfr}, y^k_{rfr}\right]^T (1 \leq k \leq K)$, respectively. Therefore, the distance between the base station and the STAR-RIS link was $d_{BR} = \sqrt{\|w_R - w_{BS}\|^2 + (H_R - H_B)^2}$, that between the STAR-RIS and reflective user link was $d^{rfl}_{RU} = \sqrt{\left\|w_R - w_{rfl}\right\|^2 + H_R^2}$, and that between the STAR-RIS and refractive user link was $d^{rfr}_{RU} = \sqrt{\left\|w_R - w_{rfr}\right\|^2 + H_R^2}$.

STAR-RIS comprises $M * N$ reflection cells, where the number of cells carrying the transmitted signal was $1 \leq m \leq M * N$. The reflection and refraction coefficients of the cells are defined as R_m and T_m, respectively. In addition, the phase shift coefficients of the reflection and refraction users were θ^{rfl}_m and θ^{rfr}_m. Therefore, the reflection and refraction signals of the m-th cell are described as follows:

$$R_m = \sqrt{\beta^{rfl}_m} e^{j\varphi^{rfl}_m}, \tag{1}$$

$$T_m = \sqrt{\beta^{rfr}_m} e^{j\varphi^{rfr}_m}, \tag{2}$$

where $\varphi^{rfl}_m, \varphi^{rfr}_m \in [0, 2\pi)$ and $\beta^{rfl}_m, \beta^{rfr}_m$ denote the energy coefficients of the reflected and refracted links, respectively. The energy consumption was negligible owing to the passive STAR-RIS. The constraint $|R_m|^2 + |T_m|^2 \leq 1$ was obtained using the ES protocol [18], i.e., $\beta^{rfl}_m + \beta^{rfr}_m \leq 1$.

Furthermore, we assumed that the three links from the base station to STAR-RIS, from STAR-RIS to the reflected user as well as the refracted user conform to the Rician distribution. In addition, the small-scale fading of the three links are defined as $h_{BR,m}$, $h^{rfl}_{RU,m}$, and $h^{rfr}_{RU,m}$, respectively.

$$\begin{aligned} \left|h^{rfl}_{RU,m}\right| &= \left|\mathbf{H}^{\mathbf{rfl}}_{\mathbf{RU}} \boldsymbol{\Theta}_{\mathbf{rfl}} \mathbf{H}_{\mathbf{BR}}\right|, \\ \left|h^{rfr}_{RU,m}\right| &= \left|\mathbf{H}^{\mathbf{rfr}}_{\mathbf{RU}} \Theta_{\mathbf{rfr}} \mathbf{H}_{\mathbf{BR}}\right|, \end{aligned} \tag{3}$$

where $\boldsymbol{\Theta}_{\text{rfl}} = \text{diag}\left[\sqrt{\beta_1^{rfl}}e^{j\phi_1^{rfl}}, \cdots, \sqrt{\beta_N^{rfl}}e^{j\phi_M^{rfl}}\right]$ denotes the diagonal matrix of the reflected link, $\boldsymbol{\Theta}_{\text{rfr}} = \text{diag}\left[\sqrt{\beta_1^{rfr}}e^{j\phi_1^{rfr}}, \cdots, \sqrt{\beta_N^{rfr}}e^{j\phi_M^{rfr}}\right]$ represents the diagonal matrix of the refracted link. $\mathbf{H}_{\mathbf{RU}}^{\mathbf{rfl}} = \left[h_{RU,1}^{rfl}, h_{RU,2}^{rfl}, \cdots, h_{RU,M}^{rfl}\right]^T$, $\mathbf{H}_{\mathbf{RU}}^{\mathbf{rfr}} = \left[h_{RU,1}^{rfr}, h_{RU,2}^{rfr}, \cdots, h_{RU,M}^{rfr}\right]^T$, and $\mathbf{H}_{\mathbf{BR}} = \left[H_{BR,1}, H_{BR,2}, \cdots, H_{BR,M}\right]^T$.

Therefore, the path losses of the three links were L_{BR}, L_{RU}^{rfl}, and L_{RU}^{rfr}. The specific mathematical relations are expressed below:

$$L_{BR} = C_{BR}\left\|X_R\right\|^{-\alpha_t} = C_{BR}d_{BR}^{-\alpha_t}, \tag{4}$$

$$L_{RU}^{rfl} = C_{RU}^{rfl}\left\|X_R - X_{RU}^{rfl}\right\|^{-\alpha_t} = C_{RU}^{rfl}d_{RU}^{rfl\ -\alpha_t}, \tag{5}$$

$$L_{RU}^{rfr} = C_{RU}^{rfr}\left\|X_R - X_{RU}^{rfr}\right\|^{-\alpha_t} = C_{RU}^{rfr}d_{RU}^{rfr\ -\alpha_t}, \tag{6}$$

where $C_{BR}, C_{RU}^{rfl}, C_{RU}^{rfr}$ satisfies $\left\{C_{BR}, C_{RU}^{rfl}, C_{RU}^{rfr}\right\} = \left(\frac{c/f_c}{4\pi d}\right)^2$ and d is defined as the standard distance (1 m); $c = 3 \times 10^8$ m/s (speed of light); f_c denotes the carrier frequency; α_t indicates the user's path-loss factor.

Moreover, We assume that the communication model operates under NOMA. Different NOMA clusters are allocated to orthogonal resource blocks, allowing us to neglect inter-cluster interference. In addition, we perform Successive Interference Cancellation (SIC) on reflective users, and STAR-RIS can adjust power allocation coefficients through an ES (Exponential Scaling) protocol. To enhance the power received by reflective users, we define the Signal-to-Interference-plus-Noise Ratio (SINR) for the SIC process of reflective users as follows:

$$\gamma_{SIC} = \frac{a_{rfl}P_tL_{BR}L_{RU}^{rfl}\left|g_m^{rfl}\right|^2}{a_{rfr}P_tL_{BR}L_{RU}^{rfl}\left|g_m^{rfl}\right|^2 + \sigma^2}, \tag{7}$$

where a_{rfl}, a_{rfr} denotes the power allocation factor ($a_{rfl} + a_{rfr} = 1$ and $a_{rfl} < a_{rfr}$); P_t indicates the power transmitted by the base station; θ^2 represents the noise power of Gaussian white noise. Accordingly, we considered that all channels conformed to Rician flat fading, and the channel power gain was $\left|g_m^i\right|^2, i = \{rfl, r\ fr\}$, conforming to the probability density function (PDF) $f_{\left|g_m^i\right|^2}(x) = \frac{1}{\lambda_i}e^{-\frac{x}{\lambda_i}}$, where λ_i denotes the mean value of $\left|g_m^i\right|^2$.

The SNR of the reflected user can be described as

$$\gamma_{rfl} = \frac{a_{rfl}P_tL_{BR}L_{RU}^{rfl}\left|g_m^{rfl}\right|^2}{\sigma^2}, \tag{8}$$

whereas the SNR of the refracted user was described as

$$\gamma_{rfr} = \frac{a_{rfr}P_tL_{BR}L_{RU}^{rfr}\left|g_m^{rfr}\right|^2}{a_{rfl}P_tL_{BR}L_{RU}^{rfr}\left|g_m^{rfr}\right|^2 + \sigma^2}. \tag{9}$$

Thus, the user system sum rate in the UAV-borne STAR-RIS-assisted NOMA system was described as

$$R = \sum_{e=1}^{E}\log(1+\gamma), \quad \left(\gamma_{SIC}, \gamma_{rfl}, \gamma_{rfr}\right) \in \gamma. \tag{10}$$

III. POWER ALLOCATION ALGORITHM

A. PROBLEM MODEL

Owing to the power limitation of STAR-RIS, the sum rate of the system needs to be maximized to ensure efficient resource utilization. Therefore, the mechanism of deploying the STAR-RIS and adjusting its power allocation factors for several users needs to be investigated under fixed user positions to maximize the sum rate of all users in the system. Based on the aforementioned model, we developed an optimal model for controlling the power allocation between the STAR-RIS and users. The objective of the proposed model is to optimize the system's sum rate and balance the load distribution among the reflective components, all the while ensuring that the communication needs of both the refractive and reflective users are satisfied. The optimization problem is formulated as follows:

$$\begin{aligned}
&\max R = \sum_{a=1}^{M}\sum_{b=1}^{N} log\left(1+\gamma_{SIC}\right) + \sum_{a=1}^{M}\sum_{b=1}^{N} log\left(1+\gamma_{rfr}\right)\\
&\min P = \frac{1}{M}\sum_{a=1}^{M}\left(\sum_{b=1}^{N}\sum_{c=1}^{S}\rho_{abc}\bar{u}_c - \sum_{a=1}^{M}\sum_{b=1}^{N}\sum_{c=1}^{S}c\bar{u}_c\right)^2\\
&C1 \quad \sum_{a=1}^{M}\sum_{b=1}^{N}\rho_{abc}log(1+\gamma) \geq u_cR_{th}, \forall c\\
&C2 \quad \beta_m^{rfl} + \beta_m^{rfr} \leq 1\\
&C3 \quad \beta_m^{rfl} \geq 0, \beta_m^{rfr} \geq 0\\
&C4 \quad \sum_{c=1}^{S}\rho_{abc} \leq 1, \forall a, b\\
&C5 \quad \overline{u_c} = u_c/\sum_{a=1}^{M}\sum_{b=1}^{N}\rho_{abc}, \forall c\\
&C6 \quad \rho_{abc} \in \{0,1\}, \forall a, b, c\\
&C7 \quad 0 \leq H_t \leq H_{\max}\\
&C8 \quad \gamma_{SIC} > \gamma_{th}^{SIC}, \gamma_{rfl} > \gamma_{th}^{out}, \gamma_{rfr} > \gamma_{th}^{out},
\end{aligned} \tag{11}$$

where the first objective function R describes the maximum sum rate to be achieved; the second objective function P represents the load variance of the reflective elements of STAR-RIS to be minimized, with the load of the elements expressed as the number of associated users; The parameter denoted as $C1$ represents the minimum rate necessary to fulfill the communication necessities of the users. This factor is of utmost importance, as it ensures that the users can transmit and receive information at a satisfactory level. $C2$ and $C3$ represent the power allocation factor constraint; $C4$ denotes the beam constraint, where each beam can cover only a single cluster of users; $C5$ indicates the load balancing constraint. When a cluster user is under coverage from multiple beams, the load is equally allocated to multiple beams covering that cluster; $C6$ denotes the associated variable ρ_{abc} (either 0 or 1); $C7$ denotes the position constraint, indicating that the deployment height of STAR-RIS cannot exceed the maximum value H_{max}. $C8$ represents the outage probability constraint. If the sub-constraint is not satisfied, link outage will occur.

B. ITERATIVE OPTIMIZATION SOLUTION MODEL

As Problem (11) is a multi-objective mixed-integer non-convex optimization model with continuous and integer variables coupled together, it cannot be easily solved using convex optimization methods. Thus, this study employed an iterative optimization method to decompose the multi-objective nonconvex model into three subproblems, namely, cluster association, power allocation, and position deployment of STAR-RIS, which were solved by considering two sets of variables within them. First, the power allocation and position-solving cluster associated variables of STAR-RIS were set. Consequently, a series of optimizations were conducted to alternate between power allocation and position adjustments in order to maximize the sum rate of the system, taking into account the resulting associations. This method of optimization was executed with great care and precision to ensure the highest possible level of performance for the system.

1) CLUSTER ASSOCIATION PROBLEM

In this section, we formulated the position of the STAR-RIS and the power allocation to multiple users. Consequently, the issue at hand is converted into a cluster association problem whereby the main aim is to achieve load balancing across the various reflective components of STAR-RIS. All this is done while ensuring that the minimum communication rate between the users is met, thus adhering to the relevant constraint:

$$
\begin{aligned}
&\min P = \frac{1}{M}\sum_{a=1}^{M}\left(\sum_{b=1}^{N}\sum_{c=1}^{S}\rho_{abc}\overline{u_c} - \sum_{a=1}^{M}\sum_{b=1}^{N}\sum_{c=1}^{S} c\overline{u_c}\right)^2 \\
&C1 \quad \sum_{a=1}^{M}\sum_{b=1}^{N}\rho_{abc} log(1+\gamma) \geq u_c\gamma_{th}, \quad \forall c \\
&C2 \quad \sum_{c=1}^{S}\rho_{abc} \leq 1, \quad \forall a, b \\
&C3 \quad \overline{u_c} = u_c / \sum_{a=1}^{M}\sum_{b=1}^{N}\rho_{abc}, \quad \forall c \\
&C4 \quad \rho_{abc} \in \{0, 1\}, \quad \forall a, b, c.
\end{aligned} \tag{12}
$$

As this problem is NP-hard, a metaheuristic algorithm was applied to solve it. Before solving, the problem was first transformed and the constraints were transformed into the objective function using the exterior penalty function [19]. Thereafter, it was transformed into the unconstrained problem as follows:

$$
\begin{aligned}
&\min \quad f(\rho) + \sum_{c}^{S}\eta_c\left[\min\left(0, h_c(\rho)\right)\right]^2 \\
&C1 \quad \sum_{c=1}^{S}\rho_{abc} \leq 1, \quad \forall a, b \\
&C2 \quad \rho_{abc} \in \{0, 1\}, \quad \forall a, b, c,
\end{aligned} \tag{13}
$$

where

$$
\begin{aligned}
f(\rho) = &\frac{1}{M}\sum_{a=1}^{M}\left(\sum_{b=1}^{N}\sum_{c=1}^{S}\rho_{abc}\left(u_c / \sum_{a=1}^{M}\sum_{b=1}^{N}\rho_{abc}\right)\right) \\
&- \frac{1}{M}\sum_{a=1}^{M}\sum_{b=1}^{N}\sum_{c=1}^{S}\rho_{abc}\left(u_k / \sum_{a=1}^{M}\sum_{b=1}^{N}\right)^2,
\end{aligned} \tag{14}
$$

$$
h_c(\rho) = \left(\sum_{a=1}^{M}\sum_{b=1}^{N}\rho_{abc} log(1+\gamma)\right) - u_c\gamma_{th}. \tag{15}
$$

In Eq.(13), η_c indicates the penalty factor, for which a value approximating 1 indicates a higher degree of approximation. According to Eq.(12) $C1$, $h_c(\rho)$ should satisfy $h_c(\rho) \geq 0$; otherwise, the objective function is subjected to a large penalty and not selected for this solution.

The Harris Hawk Optimization (HHO) algorithm is a form of swarm intelligence optimization that emulates the predatory conduct of the Harris Hawk [20]. The HHO algorithm is typically employed to solve near-optimal solutions owing to its strong global search capability. In this study, the problem in Eq.(13) was solved by improving the HHO algorithm (IHHO). The primary improvements are as follows:

(1) Improvements to initialized populations

Most intelligent-body algorithms use randomly generated population positions due to the unavailability of a priori knowledge. Herein, an initial solution was computed using the Chan algorithm that exhibits low computational complexity. Subsequently, an individual was randomly selected from the generated initial population and replaced with the initial solution to obtain the improved initial population. The improved population position was more proximate to the final optimization, thereby diminishing the global search space to achieve fast convergence. The positions of the individuals in the initial population were randomly generated as

$$
X = \text{rand}(1, 2, \cdots N) \times \left(\mathbf{u^b} - \mathbf{l^b}\right) + \mathbf{l^b} \tag{16}
$$

where $\text{rand}(1, 2, \cdots, N)$ denotes an N-dimensional random vector, and the elements are random numbers in the interval $[0, 1]$.The upper bound of the search space is $\mathbf{u^b} = [u_1^b, u^b, \cdots, u_N^b]$, and the lower bound is $\mathbf{l}^b = [l_1^b, l^b, \cdots, l_N^b]$.

(2) Improvement to the position update equation

In this study, the spiral equation is introduced in the search phase of the HHO algorithm to update the positions of

Harris Hawks, which enhanced the search capability of the original algorithm [21].As the frequency of iterations grows, the global influence of Rabbit is enhanced. This process accelerated the movement of other Harris Hawks toward Rabbit, thereby enhancing the convergence of the algorithm. The position update equation of the IHHO algorithm is expressed as

$$X(\tau+1) = |X_{\text{rabbit}}(\tau) - X(\tau)| \cdot e^{bl} \cdot \cos(2\pi l) + \left(1 - \frac{\tau^3}{T^3}\right) \cdot X_{\text{rabbit}}(\tau) \tag{17}$$

where b denotes the logarithmic spiral-shape constant and l indicates a random number on the interval $[-1,1]$.

Algorithm 1 IHHO-Based Cluster Associated Variable Algorithm

1: Initialize the prey position information and set the maximum number of iterations according to Eq.(16)
2: **while** $i < Iters$ **do**
3: Calculate the fitness of Harris Hawk
4: **for all** all Harris Hawk individuals **do**
5: Calculate the individual fitness
6: Update Harris Hawk position based on the IHHO algorithm
7: **end for**
8: **end while**
9: Output the association between the beam and the cluster

2) POWER ALLOCATION PROBLEM

In this section, we set the beam-to-cluster associations and the position of STAR-RIS. Accordingly, the issue at hand underwent a transformation into a power allocation problem, with the objective of maximizing the overall system sum rate, while also ensuring that the minimum communication rate between users is met. This approach was taken to address the aforementioned problem.

$$\begin{aligned} \max \quad & R = \sum_{a=1}^{M}\sum_{b=1}^{N} log(1+\gamma_{SIC}) + \sum_{a=1}^{M}\sum_{b=1}^{N} log(1+\gamma_{rfl}) \\ C1 \quad & \sum_{a=1}^{M}\sum_{b=1}^{N} \rho_{abc} log\big(1+\gamma\big) \geq u_c\gamma_{th}, \forall c \\ C2 \quad & \beta_m^{rfl} + \beta_m^{rfr} \leq 1 \\ C3 \quad & \beta_m^{rfl} \geq 0, \beta_m^{rfr} \geq 0 \end{aligned} \tag{18}$$

Owing to the nature of the concave function, this problem cannot be solved directly using the convex optimization methods. Based on the SNR formula and Eq.(18), let

$$h(\beta_m^{rfl}) = u_c\gamma_{th} - \sum_{a=1}^{M}\sum_{b=1}^{N} \rho_{abc} log\big(1+\gamma\big). \tag{19}$$

Upon performing the Taylor expansion of $h(\beta_m^{rfl})$ at $\beta_m^{rfl} = \beta_m^{rfl'}$, the following equation holds at all instances:

$$\begin{aligned} h(\beta_m^{rfl}) &\leq h(\beta_m^{rfl'}) + h'(\beta_m^{rfl'})(\beta_m^{rfl} - \beta_m^{rfl'}) \\ &= h^{ub}(\beta_m^{rfl}). \end{aligned} \tag{20}$$

Thus, the problem can be transformed into

$$\begin{aligned} \max \quad & R = \sum_{a=1}^{M}\sum_{b=1}^{N} log(1+\gamma_{SIC}) + \sum_{a=1}^{M}\sum_{b=1}^{N} log(1+\gamma_{rfr}) \\ C1 \quad & h^{ub}(\beta_m^{rfl}), \forall c \\ C2 \quad & \beta_m^{rfl} + \beta_m^{rfr} \leq 1 \\ C3 \quad & \beta_m^{rfl} \geq 0, \beta_m^{rfr} \geq 0 \end{aligned} \tag{21}$$

which can be considered as the upper bound for the problem stated in Eq.(18). In particular, it is a convex optimization problem, and all objective functions and constraints were related to the variable β_m^{rfl} to be optimized. Therefore, the interior point method was applied, followed by successive convex approximations to approximate the solution [22], which yielded the local optimal solution of the problem. The iterative execution of the continuous-convex-approximation power-allocation algorithm based on the interior point method is summarized in the following table.

Algorithm 2 Continuous Convex Approximation Power Allocation Algorithm Based on Interior Point Method

1: Initialize the power allocation factor $\beta_m^{rfl'}$ and the maximum number of iterations $Iters2$ satisfying the constraints
2: **while** $j < Iters2$ **do**
3: Solve problem (21) by the interior point method to obtain the optimal power allocation factor β_m^{rfl*}
4: Update power allocation factor
5: **end while**
6: Output the optimal power allocation factor for problem (18)

3) POSITION DEPLOYMENT PROBLEM

In this section, beam-to-cluster association and the power allocation of STAR-RIS to different users were fixed. Accordingly, the problem was transformed into a problem of deploying STAR-RIS at positions in which the minimum communication rate between the users was satisfied to maximize the system sum rate:

$$\begin{aligned} \max \quad & R = \sum_{a=1}^{M}\sum_{b=1}^{N} log(1+\gamma_{SIC}) + \sum_{a=1}^{M}\sum_{b=1}^{N} log(1+\gamma_{rfr}) \\ \min \quad & P = \frac{1}{M}\sum_{a=1}^{M}\left(\sum_{b=1}^{N}\sum_{c=1}^{S} \rho_{abc}\overline{u}_c - \sum_{a=1}^{M}\sum_{b=1}^{N}\sum_{c=1}^{S} c\overline{u}_c\right)^2. \end{aligned}$$

$$\begin{aligned} &C1 \quad \sum_{a=1}^{M}\sum_{b=1}^{N}\rho_{abc}log\left(1+\gamma\right) \geq u_c\gamma_{th}, \forall c \\ &C2 \quad 0 \leq H_t \leq H_{max} \end{aligned} \tag{22}$$

According to Eqs.(7)-(9), the objective function was influenced by the position of the STAR-RIS, i.e., the distance of the STAR-RIS from the base station and the users, considering the association variables and the power allocation factor. Therefore, we need to determine only the minimum communication sum rate that maximizes each user in a feasible solution satisfying the previous two subproblems. Therefore, the problem can be transformed into

$$\max \sum_{c=1}^{s}[\varphi(\phi(X_R))\phi(X_R)], \tag{23}$$

where

$$\phi(X_R) = \sum_{a=1}^{M}\sum_{b=1}^{N}\omega\rho_{abc}log\left(1+\gamma\right) - u_c\gamma_{th}, \tag{24}$$

$$\varphi(\phi(X_R)) = \begin{cases} 1, & \phi(X_R) \geq 0 \\ \upsilon, & \phi(X_R) < 0 \end{cases}. \tag{25}$$

In Eq.(24), ω satisfies $\omega = k : \rho_{abc} = 1, k \in S$, where S denotes the set of all users. Thus, ω can be considered a binary-based information for all users covered by the c beams of STAR-RIS.

The simplified position deployment problem can be solved using the improved artificial fish swarm algorithm (IAFSA) [23]. As the position of the user is known, the initial position of the STAR-RIS can be initialized based on the user position using the K-means clustering algorithm [24].

Initially, the IAFSA is an improvement on artificial fish swarm algorithm (AFSA), which enhances the iteration formula to achieve self-adaptation (Eq.(26)). Thereafter, the moving step length is improved to accelerate the convergence and improve the optimization accuracy (Eq.(27)).

$$\begin{aligned} V_t &= \varphi \cdot V_{t-1} + V_{min} \\ \varphi &= \exp\left(-\lambda\left(t/T_{max}\right)^{\tau}\right), \end{aligned} \tag{26}$$

$$F_t = \psi \cdot V_t + F_{min}, \tag{27}$$

where t denotes the number of current iterations, V_{min} represents the minimum search field of view, φ indicates the nonlinear dynamic change weight, T_{max} denotes the maximum number of iterations, λ indicates a constant, τ represents a positive integer > 1, $\psi \in (0, 1)$ denotes the control factor, and F_{min} indicates the minimum moving step length.

The specific steps for solving the problem using the IAFSA are shown in Algorithm 3.

C. ITERATIVE OPTIMIZATION ALGORITHM

Based on the solution of the three subproblems discussed earlier, this study proposed an iterative algorithm of alternate optimization to jointly optimize the cluster association, power allocation, and position deployment. After determining the cluster association relationship, the power allocation and position deployment were alternately optimized by multiple iterations to finally maximize the total sum rate of the system.

Algorithm 3 STAR-RIS Position Deployment Algorithm Based on IAFSA

1: Initialize the position of STAR-RIS using K-means algorithm and set the maximum number of iterations G
2: **while** $g < G$ **do**
3: Calculate individual fitness and execute behavior according to rules
4: Select the individual with the maximum value in the objective function
5: **end while**
6: Output the position coordinates of problem (23)

The following is the basic workflow of the algorithm:

Initialization parameters: We first initialize the parameters of the system. This includes determining the location and power allocation scheme of STAR-RIS, and defining cluster association.

Fixed power allocation and location for solving cluster correlation: In the first round of iteration, we choose fixed power allocation and location, and solve the cluster correlation problem.

Alternating optimization of power allocation and location: Once the cluster correlation is determined, we start alternating optimization of power allocation and location. Specifically, we first fix the position and solve the power allocation problem to maximize the sum rate of the system. Then, we fix the power allocation and optimize the location of STAR-RIS according to the current power allocation to further improve the sum rate. This alternating process is repeated until it converges or reaches a predetermined number of iterations.

Iterative termination condition: We set a termination condition in the algorithm. When the algorithm converges to a stable state and satisfies the termination condition, the algorithm stops and returns the optimal power allocation, location and cluster association.

Algorithm 4 is the pseudo-code of alternating iterative algorithm.

As observed, the variables derived using the proposed iterative optimization algorithm were not necessarily globally optimal. Moreover, the variables were influenced by the initialization values.

IV. SIMULATION ANALYSIS

In this section, we performed MATLAB simulations to evaluate the power allocation algorithm's performance for the joint position of the STAR-RIS-assisted NOMA system. The simulations aimed to assess the sum rate performance of the user system. We assumed a communication environment with dimensions of $1000m \times 1000\ m \times 200\ m$. The area contained 100 communication users, and the base station

Algorithm 4 Iterative Algorithm With Alternate Optimization

Initialize the base station, STAR-RIS, user's position and beam power of the reflecting element
while each user meets the minimum communication rate and the link communicates properly **do**
    Fix the power allocation factor and the position of STAR-RIS and calculate the cluster correlation according to Algorithm 1
    Calculate the sum rate of the system
    while sum rate threshold **do**
        Fix the power allocation factor and cluster association and optimize the position deployment according to Algorithm 3
        Fix cluster association and STAR-RIS positions and optimize the power allocation according to Algorithm 2
        Calculate the sum rate of the system
    end while
    Calculate the user's communication rate
end while
Output cluster associations, power allocation factors and STAR-RIS positions

utilized 4 antennas with a bandwidth of 10 MHz. The STAR-RIS consisted of 20 reflective cells, and the path loss factor was set to 2.4. The power distribution factor was denoted as $\beta_{rfl} + \beta_{rfr} = 1$, and certain parameters were derived from the existing literature [25]. Three different types of user distributions (uniform, normal, and Poisson) are discussed to simulate three different types of communication environment requirements. The users are divided into q clusters according to the coverage of the beam, using the clustering method in the literature [26]. What we use is power domain NOMA. The SCMA and PDMA proposed in literature [27] can effectively improve the spectrum efficiency. SCMA or PDMA can be considered in subsequent work. The following table lists the main parameters used in this study.

TABLE 1. Simulation parameter table.

Parameter name and Parameter symbol	Value
Number of users U	100
Number of base station antennas J	4
Number of STAR-RIS components M	20
Number of user clusters c	9
Meet the user's minimum communication rate R_{th}	$0.15bit/s/Hz$
Path loss factor α_t	2.4
Base station transmitting power P_t	$30dBm$
UAV weight W_U	$3.25Kg$
STAR-RIS Element W_E	$7.66 * 10^{-3}Kg$
Battery weight W_B	$1.35Kg$

To facilitate the simulation, the STAR-RIS elements were segmented into four blocks according to their respective regions: top-left, bottom-left, top-right, and bottom-right. The simulation investigated the relationship between the number of clusters and the load disparity of STAR-RIS elements across various user distributions (Figure 3). Notably, the load differences among components in each region displayed negligible significance as observed in Figure 3. Specifically, under a uniform distribution of users, the element load differences were minimal. However, in the Gaussian and Poisson distribution modes, where user concentration was higher compared to the uniform distribution, a greater number of users tended to access the same area element, leading to load imbalance. Regardless of any specific user distribution, the load difference between the components decreased with an increasing number of user clusters increased, which consequently segmented the users into fine groups, resulting in a more balanced distribution of user access. To prevent excessive user concentration or dispersion, the communication system adopted clustering rules to divide the users into clusters.

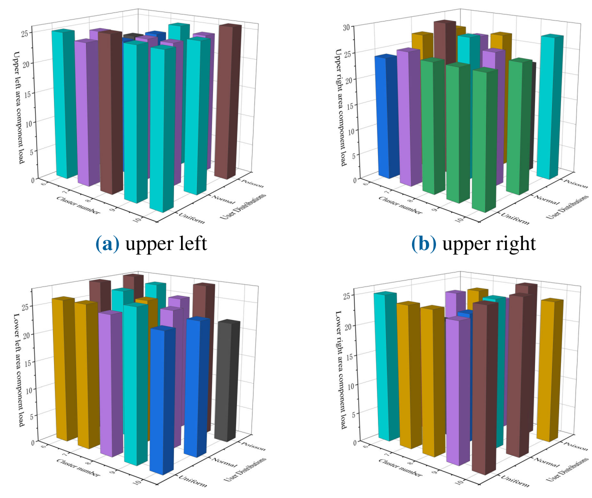

(a) upper left (b) upper right
(c) lower left (d) lower right

FIGURE 3. Difference in STAR-RIS component load across number of clusters and various user distributions.

When the users are divided into 9 clusters. Accordingly, for subsequent experiments, the experimental environment is configured with 9 clusters. The disparities in STAR-RIS component loads across different user distributions are illustrated in Figure 4. Under a uniform distribution, the load differences between the components were minimized because of the homogeneous user distribution. In contrast, the Gaussian distribution, simulating an urban environment, exhibited greater user concentration, yielding more pronounced load differences. Conversely, the Poisson distribution, representing a rural environment, displayed user size aggregation, which caused the largest variation in component loads compared to the uniform distribution.

To validate the effectiveness of the proposed algorithm in addressing the user association problem and achieving component load balancing, this study compared the STAR-RIS component load differences between the IHHO

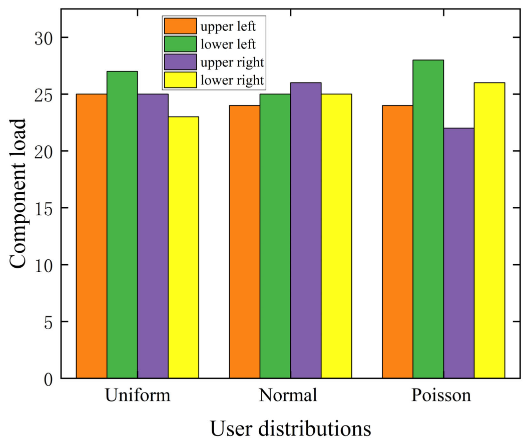

FIGURE 4. Difference in STAR-RIS component load under various user distributions.

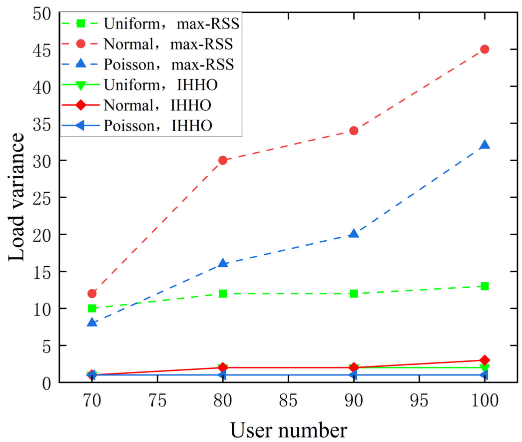

FIGURE 5. Difference in STAR-RIS component loadings between the IHHO and max-RSS algorithms.

algorithm and the max-RSS algorithm [28]. Additionally, the analysis examined the load differences between the STAR-RIS elements under varying user numbers and distributions.

Figure 5 showcases the component load differences, with the dashed lines representing the max-RSS algorithm and the solid lines representing the IHHO algorithm. Notably, all solid lines in the figure exhibit significantly lower values compared to the dashed lines, indicating the superior load balancing achieved by the proposed IHHO algorithm. Furthermore, as the number of users increased, the slope of the dashed line became steeper than that of the solid line, highlighting the advantage of the proposed algorithm in scenarios with larger user counts.

Following the iteration of the IHHO algorithm, the load differences among STAR-RIS elements are equalized. The subsequent step involves optimizing the power allocation of STAR-RIS. With the associations and positions fixed, the objective is to maximize the system sum rate for each user while ensuring a minimum communication rate.

Figure 6 depicts the changes in system sum rate when using the average distribution algorithm (represented by the dashed line) and the algorithm proposed in this study

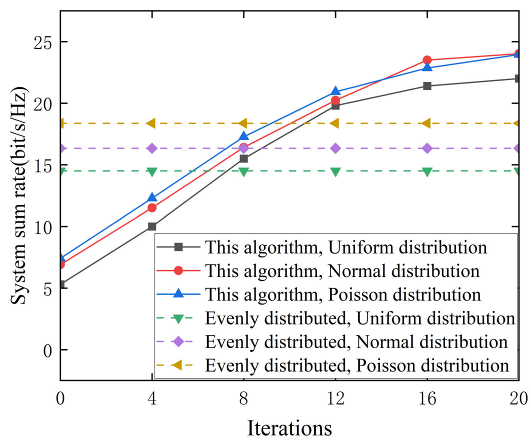

FIGURE 6. Variations in system sum rate with the number of iterations.

(represented by the solid line). The average distribution algorithm distributes power equally, resulting in a constant system sum rate throughout the iterations. In contrast, the proposed algorithm gradually increases and stabilizes the user system sum rate with each iteration. As demonstrated in Figure 6, the user system sum rates based on the proposed algorithm surpass those based on the average distribution algorithm. Specifically, the system sum rate improvements under the three different distributions are 34.1%, 32%, and 23.3%, respectively.

The performance of the position deployment algorithm proposed in this study exhibited variations based on the number of iterations, the fixed cluster association relationship, and the power allocation factor of STAR-RIS, as depicted in Figure 7. The variations in the system sum rate with the number of iterations for users conforming to a uniform distribution, Gaussian distribution, and Poisson distribution are illustrated in Figure 7(a)-(c), respectively.

As indicated in Figure 7, the user system sum rates achieved with the STAR-RIS deployment positions determined by the proposed IAFSA algorithm surpassed those obtained with the standard AFSA, Differential Evolution algorithm (DE) [29], and Particle Swarm Optimization algorithm (PSO) [30] for all three user distributions. Furthermore, the IAFSA algorithm exhibited faster convergence and a higher slope during the initial iterations, indicating superior performance compared to the other three algorithms. This advantage stems from the introduced adaptive iteration formula and moving step length, as well as the enhanced algorithm search capability, optimization-seeking accuracy, and convergence speed of the IAFSA.

To further emphasize the effectiveness of the power-allocation algorithm for the joint position deployment proposed herein, the performance of the joint optimization algorithm was compared to that of the single power optimization algorithm (Figure 8). Across the three user distributions, the joint optimization algorithm achieved improvements of 14.6%, 21.1%, and 18.0%, respectively, compared to the single-power optimization. Figure 8 highlights that the

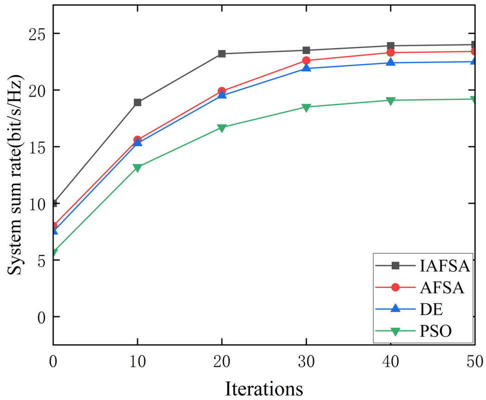

(a) Uniform distribution

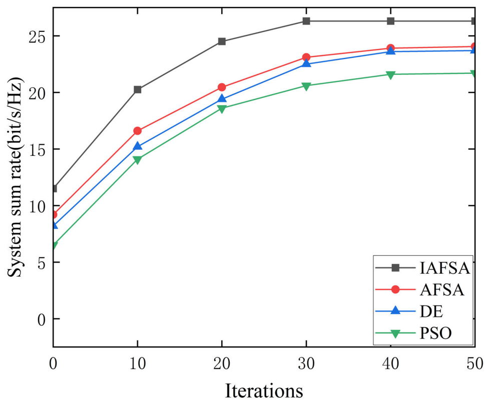

(b) Gaussian distribution

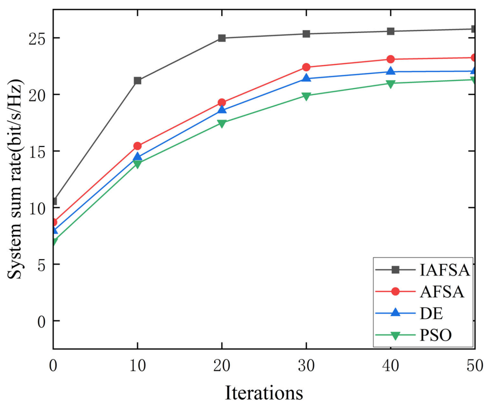

(c) Poisson distribution

FIGURE 7. System sum rate variation with the number of iterations.

user system sum rate under the joint optimization-based algorithm surpassed that under the single-power optimization algorithm, regardless of the user distribution, further affirming the effectiveness of the proposed joint optimization algorithm.

In this study, we make the assumption that users follow a Gaussian distribution, with fixed values of $\beta_{rfl} = 0.3$, $\beta_{rfr} = 0.7$, and P_{dBm} ranging from 15 to 25 dBm. The number of reflective elements considered varies between 20, 24, 28, 32, 36, and 40. The objective of our investigation is to analyze the impact of the number of STAR-RIS reflective elements on the performance of UAV-borne STAR-RIS

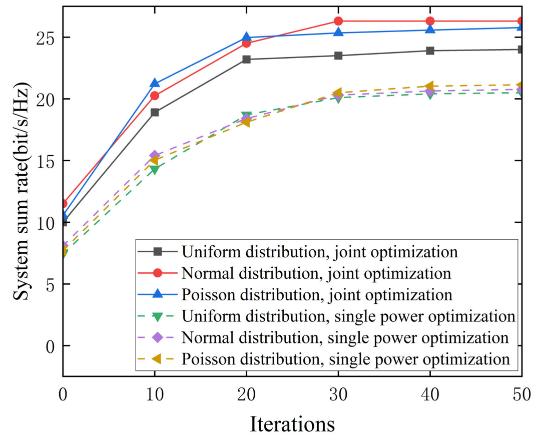

FIGURE 8. Graph of user system sum rate variation with the number of iterations.

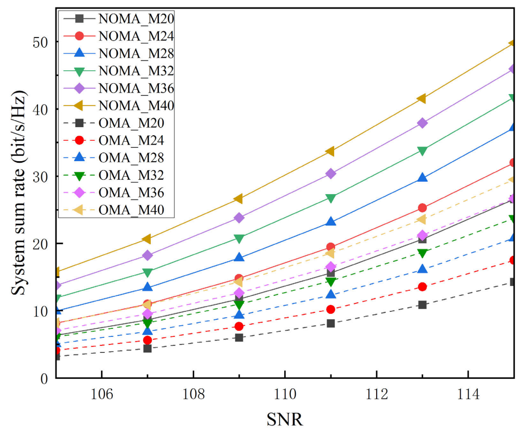

FIGURE 9. System sum rate variation with the number of STAR-RIS reflective units.

assisted NOMA communication and OMA communication systems. As depicted in Figure 9, we observe that, when the transmit power is kept constant, both the system and the rate experience an increase as the number of STAR-RIS reflective elements increases. Moreover, we note that as the reflective power increases, the rate of improvement in system performance and rate becomes more significant. Therefore, by increasing the number of STAR-RIS reflective elements within the constraints of UAV and STAR-RIS limitations, and without compromising UAV aerodynamic performance, we can effectively enhance the performance of the communication system.

Additionally, We refer to reference [31] to set the number of STAR-RIS reflective elements in the interval [20, 40] in order to analyze the system performance. We conduct a comparison between the performance of the UAV-borne STAR-RIS system in NOMA and OMA communication systems. From the graph, it is evident that, when the reflective power is fixed, NOMA-assisted STAR-RIS communication surpasses OMA-assisted STAR-RIS communication, resulting in an average improvement of 2.01 times in both system and rate.

V. CONCLUSION

This study investigated the joint optimization problem of the UAV-borne STAR-RIS-assisted NOMA system, aiming to optimize the cluster associations, power allocation factors, and STAR-RIS positions for maximizing the system sum rate for users. To address the nonconvex optimization problem, we proposed an alternating iterative joint optimization algorithm that iteratively solved the joint optimization problem of cluster association relationships, power allocation factors, and STAR-RIS positions. The effectiveness of the proposed UAV-borne STAR-RIS-assisted NOMA system was validated based on simulation results.The algorithm we propose manages to maximize the number of the sum rate of the system, resulting in a significant 31.6% improvement when compared to the single-power optimization algorithm.

The alternating iteration-based joint optimization algorithm proposed in this study contributes toward optimizing UAV-borne STAR-RIS systems, which will benefit applications in wireless communication, IoT, and smart cities. In future research, we intend to delve deeper into the joint design of beamforming, and phase shift optimization for UAV-borne STAR-RIS.

VI. ABBREVIATIONS

See Table 2.

TABLE 2. Table of abbreviations.

Abbreviation	Full name
RIS	Reconfigurable Intelligent Surface
STAR-RIS	Simultaneous Transmitting and Reflecting RIS
NOMA	Non-Orthogonal Multiple Access
OMA	Orthogonal Multiple Access
NLOS	Non-Line-of-Sight
LOS	Line-of-Sight
UAV	Unmanned Aerial Vehicle
ES	Energy Splitting
MS	Mode Switching
TS	Time Switching
KKT	Karush Kuhn Tucke
UPA	Uniform Planar Array
SIC	Successive Interference Cancellation
HHO	Harris Hawk Optimization
IHHO	Improverd Harris Hawk Optimization
IAFSA	Improved Artificial Fish Swarm Algorithm
DE	Differential Evolution Algorithm
PSO	Particle Swarm Optimization algorithm

ACKNOWLEDGMENT

The authors would like to thank the Yunnan Key Laboratory of Computer Technologies Application for its support and also would like to thank (service@zhiyunwenxian.cn) for the polishing service provided to this article.

(Yi Peng and Jian Tang are co-first authors.)

REFERENCES

[1] S. Basharat, S. A. Hassan, H. Pervaiz, A. Mahmood, Z. Ding, and M. Gidlund, "Reconfigurable intelligent surfaces: Potentials, applications, and challenges for 6G wireless networks," *IEEE Wireless Commun.*, vol. 28, no. 6, pp. 184–191, Dec. 2021.

[2] M. A. ElMossallamy, H. Zhang, L. Song, K. G. Seddik, Z. Han, and G. Y. Li, "Reconfigurable intelligent surfaces for wireless communications: Principles, challenges, and opportunities," *IEEE Trans. Cognit. Commun. Netw.*, vol. 6, no. 3, pp. 990–1002, Sep. 2020.

[3] X. Mu, Y. Liu, L. Guo, J. Lin, and R. Schober, "Simultaneously transmitting and reflecting (STAR) RIS aided wireless communications," *IEEE Trans. Wireless Commun.*, vol. 21, no. 5, pp. 3083–3098, May 2022.

[4] J. Zhao, Y. Zhu, X. Mu, K. Cai, Y. Liu, and L. Hanzo, "Simultaneously transmitting and reflecting reconfigurable intelligent surface (STAR-RIS) assisted UAV communications," *IEEE J. Sel. Areas Commun.*, vol. 40, no. 10, pp. 3041–3056, Oct. 2022.

[5] C. Wu, C. You, Y. Liu, X. Gu, and Y. Cai, "Channel estimation for STAR-RIS-Aided wireless communication," *IEEE Commun. Lett.*, vol. 26, no. 3, pp. 652–656, Mar. 2022.

[6] C. Wu, Y. Liu, X. Mu, X. Gu, and O. A. Dobre, "Coverage characterization of STAR-RIS networks: NOMA and OMA," *IEEE Commun. Lett.*, vol. 25, no. 9, pp. 3036–3040, Sep. 2021.

[7] T. Wang, M.-A. Badiu, G. Chen, and J. P. Coon, "Outage probability analysis of STAR-RIS assisted NOMA network with correlated channels," *IEEE Commun. Lett.*, vol. 26, no. 8, pp. 1774–1778, Aug. 2022.

[8] J. Zuo, Y. Liu, Z. Ding, L. Song, and H. V. Poor, "Joint design for simultaneously transmitting and reflecting (STAR) RIS assisted NOMA systems," *IEEE Trans. Wireless Commun.*, vol. 22, no. 1, pp. 611–626, Jan. 2023.

[9] P. P. Perera, V. G. Warnasooriya, D. Kudathanthirige, and H. A. Suraweera, "Sum rate maximization in STAR-RIS assisted full-duplex communication systems," in *Proc. IEEE Int. Conf. Commun. (ICC)*, May 2022, pp. 3281–3286.

[10] B. Shao, M. Li, and X. Shi, "Distributed resource allocation algorithm for general linear multiagent systems," *IEEE Access*, vol. 10, pp. 74691–74701, 2022.

[11] P.-V. Mekikis, D. Tyrovolas, S. Tegos, A. Papadopoulos, A. Pitilakis, S. Ioannidis, A. Tsioliaridou, P. Diamantoulakis, N. Kantartzis, G. Karagiannidis, and C. Liaskos, "Dynamic programmable wireless environment with UAV-mounted static metasurfaces," in *Proc. IEEE Conf. Standards Commun. Netw. (CSCN)*, Nov. 2022, pp. 101–104.

[12] X. Wang, Z. Lin, F. Lin, and P. Xiao, "Quantum sensing based joint 3D beam training for UAV-mounted STAR-RIS aided TeraHertz multi-user massive MIMO systems," 2022, *arXiv:2212.07731*.

[13] Q. Zhang, Y. Zhao, H. Li, S. Hou, and Z. Song, "Joint optimization of STAR-RIS assisted UAV communication systems," *IEEE Wireless Commun. Lett.*, vol. 11, no. 11, pp. 2390–2394, Nov. 2022.

[14] A. Pitilakis, D. Tyrovolas, P.-V. Mekikis, S. A. Tegos, A. Papadopoulos, A. Tsioliaridou, O. Tsilipakos, D. Manessis, S. Ioannidis, N. V. Kantartzis, I. F. Akyildiz, and C. K. Liaskos, "On the mobility effect in UAV-mounted absorbing metasurfaces: A theoretical and experimental study," *IEEE Access*, vol. 11, pp. 79777–79792, 2023.

[15] D. Tyrovolas, P.-V. Mekikis, S. A. Tegos, P. D. Diamantoulakis, C. K. Liaskos, and G. K. Karagiannidis, "Energy-aware design of UAV-mounted RIS networks for IoT data collection," *IEEE Trans. Commun.*, vol. 71, no. 2, pp. 1168–1178, Feb. 2023.

[16] Z. Yang, W. Xu, and M. Shikh-Bahaei, "Energy efficient UAV communication with energy harvesting," *IEEE Trans. Veh. Technol.*, vol. 69, no. 2, pp. 1913–1927, Feb. 2020.

[17] Y. Xiao et al., "Solar powered UAV-mounted RIS networks," *IEEE Commun. Lett.*, vol. 27, no. 6, pp. 1565–1569, Jun. 2023, doi: 10.1109/LCOMM.2023.3264493.

[18] C. Zhang, W. Yi, Y. Liu, Z. Ding, and L. Song, "STAR-IOS aided NOMA networks: Channel model approximation and performance analysis," *IEEE Trans. Wireless Commun.*, vol. 21, no. 9, pp. 6861–6876, Sep. 2022.

[19] J. Viswanathan and I. E. Grossmann, "A combined penalty function and outer-approximation method for MINLP optimization," *Comput. Chem. Eng.*, vol. 14, no. 7, pp. 769–782, Jul. 1990.

[20] A. A. Heidari, S. Mirjalili, H. Faris, I. Aljarah, M. Mafarja, and H. Chen, "Harris hawks optimization: Algorithm and applications," *Future Gener. Comput. Syst.*, vol. 97, pp. 849–872, Aug. 2019.

[21] J. G. Pipe and N. R. Zwart, "Spiral trajectory design: A flexible numerical algorithm and base analytical equations," *Magn. Reson. Med.*, vol. 71, no. 1, pp. 278–285, Jan. 2014.
[22] M. Razaviyayn, "Successive convex approximation: Analysis and applications," Ph.D. dissertation, Univ. Minnesota, 2014.
[23] Y. Cai, "Artificial fish school algorithm applied in a combinatorial optimization problem," *Int. J. Intell. Syst. Appl.*, vol. 2, no. 1, pp. 37–43, Nov. 2010.
[24] A. Likas, N. Vlassis, and J. J. Verbeek, "The global k-means clustering algorithm," *Pattern Recognit.*, vol. 36, no. 2, pp. 451–461, Feb. 2003.
[25] B. Zhao, C. Zhang, W. Yi, and Y. Liu, "Ergodic rate analysis of STAR-RIS aided NOMA systems," *IEEE Commun. Lett.*, vol. 26, no. 10, pp. 2297–2301, Oct. 2022.
[26] N. Docomo, *Performance of eICIC With Control Channel Coverage Limitation*, Standard R1-103264, 3GPP, Montreal, QC, Canada, vol. 5, 2010, p. 27.
[27] W. Yuan, N. Wu, Q. Guo, Y. Li, C. Xing, and J. Kuang, "Iterative receivers for downlink MIMO-SCMA: Message passing and distributed cooperative detection," *IEEE Trans. Wireless Commun.*, vol. 17, no. 5, pp. 3444–3458, May 2018.
[28] B. Agarwal, M. A. Togou, M. Ruffini, and G.-M. Muntean, "A low complexity ML-assisted multi-knapsack-based approach for user association and resource allocation in 5G HetNets," in *Proc. IEEE Int. Symp. Broadband Multimedia Syst. Broadcast. (BMSB)*, Jun. 2023, pp. 1–6.
[29] K. Price, R. M. Storn, and J. A. Lampinen, *Differential Evolution: A Practical Approach to Global Optimization*. Springer, 2006. [Online]. Available: https://link.springer.com/book/10.1007/3-540-31306-0
[30] F. Marini and B. Walczak, "Particle swarm optimization (PSO). A tutorial," *Chemometric Intell. Lab. Syst.*, vol. 149, pp. 153–165, Dec. 2015.
[31] Q. Gao, Y. Liu, X. Mu, M. Jia, D. Li, and L. Hanzo, "Joint location and beamforming design for STAR-RIS assisted NOMA systems," *IEEE Trans. Commun.*, vol. 71, no. 4, pp. 2532–2546, Apr. 2023.

YI PENG received the B.Sc., M.Sc., and Ph.D. degrees from the University of Electronic Science and Technology of China, in 1996, 2001, and 2005, respectively. She is currently an Associate Professor with the School of Information Engineering and Automation, Kunming University of Science and Technology. Her research interests include wireless communication and RIS.

JIAN TANG received the B.Sc. degree from the Hunan University of Technology, in 2021. He is currently pursuing the M.Sc. degree with the School of Information Engineering and Automation, Kunming University of Science and Technology. His main research interests include emergency communication and STAR-RIS.

QINGQING YANG received the B.Sc. and M.Sc. degrees from Harbin Engineering University, in 2004 and 2007, respectively, and the Ph.D. degree from the Kunming University of Science and Technology, in 2020. She is currently a Lecturer and a Master Tutor with the School of Information Engineering and Automation, Kunming University of Science and Technology. Her main research interests include RIS and emergency communication.

ZHUOTING HAN received the bachelor's degree from the Kunming University of Science and Technology, in 2017, where he is currently pursuing the master's degree with the School of Information Engineering and Automation. His main research interests include RIS and NOMA.

JIAN MA received the bachelor's degree from Neijiang Normal University, in 2021. He is currently pursuing the master's degree with the School of Information Engineering and Automation, Kunming University of Science and Technology. His main research interests include RIS and emergency communication.